Non-Orthogonal Matrix Precoding based Faster-than-Nyquist Signaling over Optical Wireless Communications

Zhouyi Hu and Chun-Kit Chan
Department of Information Engineering, The Chinese University of Hong Kong, Shatin, N. T., Hong Kong, China
Author e-mail address: huzhouyi@ie.cuhk.edu.hk; ckchan@ie.cuhk.edu.hk

Abstract: We first investigate a novel non-orthogonal matrix precoding based faster-than-Nyquist signaling technology in OWC systems. Compared to the conventional schemes, it shows superior performance including PAPR reduction, improved sensitivity, and improved tolerance to narrow-bandwidth filtering.
OCIS codes: (060.2605) Free-space optical communication; (060.4510) Optical communications.

1. Introduction

Compared with the conventional radio frequency (RF) technology, optical wireless communications (OWC) has been an attractive solution for future high-speed wireless access, due to its high security and immunity to electromagnetic interference. Owing to the limitation of cost, OWC usually adopts intensity modulation and direct detection (IM/DD) at transmitter side and receiver side, respectively, however at the expense of spectral efficiency (SE). To increase the data rate in an OWC IM/DD system, many advanced digital signal processing (DSP) techniques have been investigated [1].

On the other hand, spectrally efficient frequency division multiplexing (SEFDM), also termed as faster-than-Nyquist non-orthogonal frequency-division multiplexing (FTN-NOFDM) has been recently proposed [2] to achieve the improved SE compared to the conventional orthogonal frequency-division multiplexing (OFDM) signal. However, since FTN-NOFDM violates the orthogonality principle of modulated subcarriers in the frequency domain directly, many issues inevitably arise. For instance, the generation of a real-valued FTN-NOFDM signal for IM/DD systems is not easy [3]. The channel estimation and equalization is also a crucial challenge for FTN-NOFDM systems due to the combined channel state information (CSI) with the purposely induced inter-channel interference (ICI). Although many schemes have been proposed [4], they inevitably increased the system complexity.

In this work, for the first time, we investigate a novel non-orthogonal matrix precoding (NOM-p) based FTN signaling technology and experimentally demonstrate it in an OWC system. A 21.82-Gb/s FTN signal with 25% bandwidth saving has been successfully transmitted over OWC, including 20.1-km standard single mode fiber (SSMF) and 2-m free-space channel, while keeping its bit error rate (BER) below the hard-decision forward error correction (HD-FEC) threshold. The experimental results also indicate its improved performance compared to both OFDM and FTN-NOFDM signals.

2. Principle

In [5], a technique, termed as FTN single carrier multiple-input/multiple-output (FTN SC-MIMO), was proposed to save bandwidth, which shared the similar behavior as FTN-NOFDM. Herein, we propose to extend the concept of FTN SC signaling to a more general case, where the matrix for precoding is not limited to discrete Fourier transform (DFT). Moreover, we further propose a multi-band (MB) architecture to reduce the complexity of decoding.

2.1. Single-Band NOM-p FTN

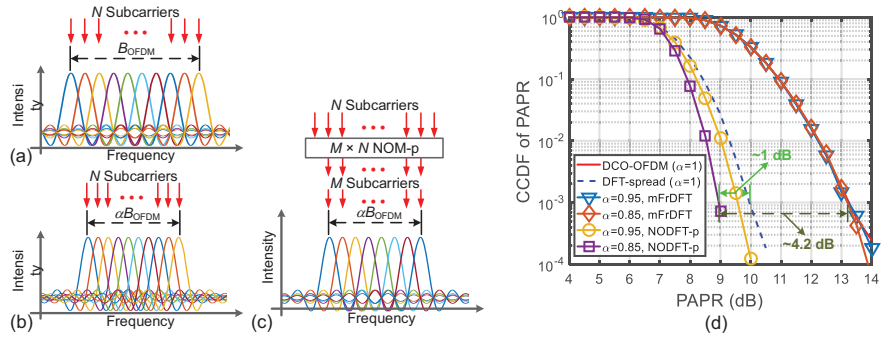

Fig. 1. Sketched spectra of (a) OFDM (α=1), (b) FTN-NOFDM (α=0.8), and (c) the proposed NOM-p FTN (α=M/N=8/10=0.8) signals. (d) CCDF of PAPR for different signals, where 120/256 subcarriers are effectively modulated by 4-QAM symbols.

Fig. 1 compares the sketched spectra of OFDM, FTN-NOFDM, and the proposed NOM-p FTN signals. We can see from Fig. 1(b) that the subcarrier spacing of the conventional FTN-NOFDM is compressed to α (< 1) of its original spacing in the OFDM depicted in Fig. 1(a). Here, α denotes the compression factor. As shown in Fig. 1(c), the main idea of NOM-p is to squeeze N subcarriers into M subcarriers by an $M\times N$ ($M\leqslant N$) transform matrix for acceleration. In this case, the compression factor is defined by $\alpha=M/N$. Note that ICI is induced by NOM-p rather than directly violating the orthogonality principle in the frequency domain. Hence, the proposed FTN signal shows a similar behavior as the conventional OFDM signal, leading to a great compatibility in terms of some advanced DSP techniques already used in OFDM. In particular, since the subcarriers are still orthogonal in the frequency domain, the implementation of channel estimation and the subsequent equalization are significantly simplified, which is still a challenge for the conventional FTN-NOFDM [4] systems.

Without loss of generality, if we use a standard DFT matrix to generate an NOM, termed as NODFT matrix W, for FTN signaling, its (m, n)-th entry is denoted by: $W_{m,n}=\exp\left(-j2\pi mn/N\right)/\sqrt{M}$, for m = 0, 1, …, M–1 and n = 0, 1, …, N–1. It can be noticed that W is equivalent to the standard DFT matrix when α = 1 (M = N). For decoding, the inverse NODFT (INODFT) matrix W^{H} is employed, which is the Hermitian transpose of W. The (i, k)-th entry of its correlation matrix C can then be calculated by: $C_{i,k}=W^{\mathrm{H}}W=\sum_{m=0}^{M-1}\exp\left(-j2\pi m(k-i)/N\right)/M$, for i, k = 0, 1, …, N–1. Note that C is not an identity matrix when $M\neq N$. The purposely induced ICI can be mitigated by the cascaded binary-phase-shift-keying iterative detection (CBID) algorithm with relatively low complexity [6].

In addition to bandwidth saving, the proposed NOM-p also provides the coding gain which originates from its orthogonal version. In Fig. 1(d), we present the complementary commutative distribution function (CCDF) of PAPR curves for different signals. Herein, we use modified fractional discrete Fourier transform (mFrDFT) to generate the conventional FTN-NOFDM signal [3]. We can see from the figure that similar to the DFT-spread OFDM [7], the proposed NODFT-p technology can significantly reduce PAPR, and even show an improved performance.

2.2. *Multi-Band NOM-p FTN*

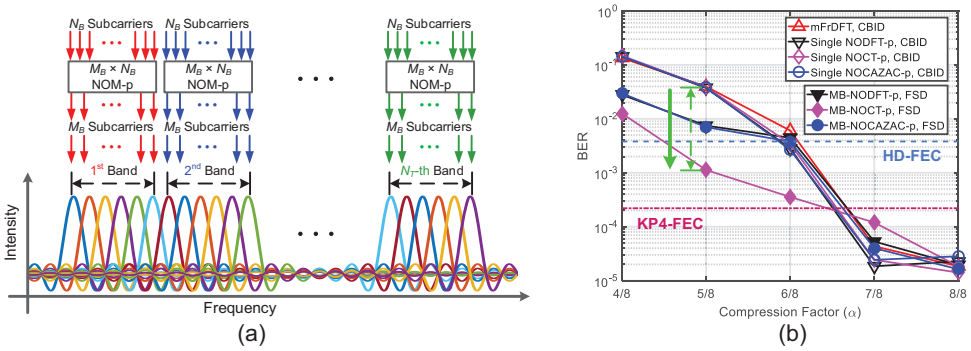

Fig. 2. (a) Procedure of the proposed MB-NOM-p FTN signaling. (b) BER versus the value of α for different FTN signals (SNR=12 dB).

Apart from CBID, several advanced soft-decision decoders can also be used for ICI elimination, such as fixed sphere decoding (FSD) [8]. However, the computational complexity of FSD exponentially increases with the number of subcarriers. To resolve this issue, we further propose a novel MB-NOM-p FTN signaling technology to reduce the complexity of FSD for supporting the large-size multi-carrier FTN system.

Fig. 2(a) illustrates the procedure of the proposed MB-NOM-p. In each sub-band, the symbols allocated on N_B subcarriers are pre-coded by a small-size NOM ($M_B \times N_B$) for FTN signaling. The resulting M_B subcarriers are then orthogonally allocated in the frequency domain with other subcarriers from different sub-bands. Since the sub-band is still orthogonal to each other in the proposed system, there is no out-of-block interference required for elimination, leading to reduced complexity and increased transmission performance [3].

The feasibility of MB-NOM-p with FSD has been verified via numerical simulations. In addition to NODFT, two other NOMs have also been investigated, including non-orthogonal circulant matrix transform (NOCT) and non-orthogonal constant amplitude zero autocorrelation (NOCAZAC) transform, which are modified from references [9] and [10], respectively. In this simulated IM/DD system, the signal-to-noise ratio (SNR) is fixed at 12 dB, and N is set to 120 for effective modulation. For MB-NOM-p FTN signals, N_B is set to 8, and the number of bands can be calculated by $N_T=N/N_B=15$. Thanks to the small size of each sub-band, we can apply the advanced FSD to the FTN signals with MB-NOM-p, at the expense of moderate complexity. For the other FTN signals, only CBID is suitable. Fig. 2(b) presents the BER curves of various FTN signals with different values of α, verifying the superior performance of the proposed MB-NOM-p FTN signaling.

3. Experimental Setup and Results

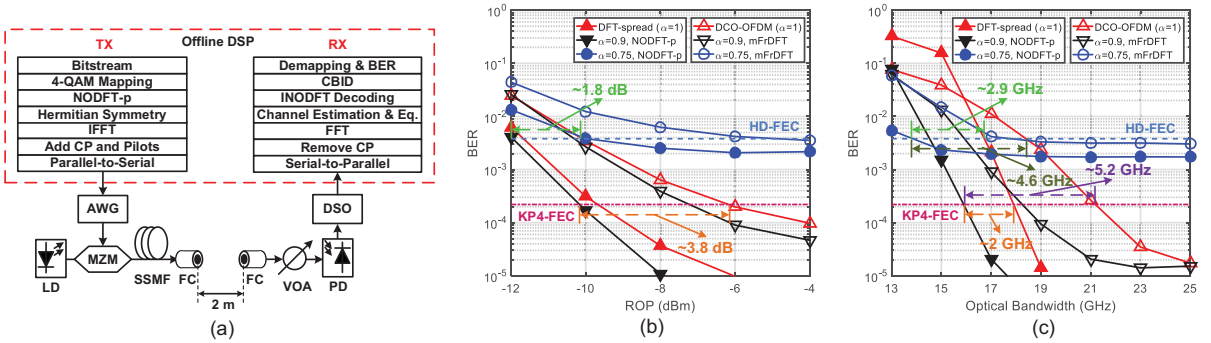

Fig. 3. (a) Experimental setup and DSP of the proposed NODFT-p FTN OWC system. Measured BER versus (b) ROP (20.1-km SSMF and 2-m free space) and (c) optical bandwidth (5.6-km SSMF and 2-m free space, ROP=3.5 dBm) for different signals.

Fig. 3(a) shows the experimental setup of OWC and the corresponding DSP. At the transmitter, the obtained 4-QAM symbols were first allocated on 120 subcarriers (N=120) and then squeezed into M subcarriers by single-band NODFT-p, according to the value of α. Hermitian symmetry was employed before performing a 256-point inverse fast Fourier transform (IFFT) so as to generate a real-valued FTN signal. The inserted cyclic prefix (CP) was 1/32 of the size of IFFT. A 24-GSa/s arbitrary waveform generator (AWG) then converted the obtained digital signal into an analog electrical signal. Hence, the data rate of these FTN signals was fixed at 21.82 Gb/s. The electrical bandwidth of different signals can also be calculated, i.e., 11.25 GHz for α = 1, 10.125 GHz for α = 0.9, and 8.4375 GHz for α = 0.75. Then, a laser diode (LD) and a Mach-Zehnder modulator (MZM) were used for external modulation in order to generate a modulated optical signal with a central wavelength at ~1550 nm. After transmitting over 20.1-km SSMF, the infrared signal was launched into 2-m free-space channel via a fiber collimator (FC). At the receiver, another FC was used for coupling with a coupling loss of ~1 dB. A variable optical attenuator (VOA) was then used to vary the received optical power (ROP) values. After detection by a photodiode (PD), the resulting electrical signal was captured by a digital storage oscilloscope (DSO) operated at 50 GSa/s for the offline DSP at receiver.

Fig. 3(b)-(c) present the experimental results. In this paper, we have also investigated DCO-OFDM, DFT-spread OFDM, and FTN-NOFDM based on mFrDFT to illustrate the advantage of the proposed FTN signaling technology. Fig. 3(b) shows the BER versus ROP for different signals. We can see that the proposed NODFT-p FTN signal always outperforms the conventional FTN-NOFDM signal with the same α, which can be attributed to its coding gain. Moreover, due to bandwidth saving, the NODFT-p signal has a higher tolerance to the bandwidth limitation induced by both chromatic dispersion and devices. Hence, when α=0.9, in spite of suffering from ICI, the NODFT-p signal can slightly outperform the DFT-spread OFDM signal. In particular, it shows ~1.8 dB and ~3.8 dB sensitivity improvements over the DCO-OFDM signal at the HD-FEC threshold and KP4-FEC threshold, respectively.

Herein, we have further investigated the tolerance to narrow-bandwidth filtering for different signals, as shown in Fig. 3(c). An optical bandpass filter was adopted after MZM to emulate the additional filtering effect induced by some optical components. The SSMF was shortened to 5.6 km to fix the ROP at 3.5 dBm. We can see that the BERs of both DCO-OFDM signal and DFT-spread OFDM signal increase rapidly at the bandwidth-limited region. However, with NODFT-p, the tolerance to filtering is increased significantly. At HD-FEC threshold, the bandwidth sensitivity improvement is up to ~2.9 GHz and ~4.6 GHz, compared to DFT-spread OFDM and DCO-OFDM, respectively. At KP4-FEC threshold, the corresponding improvements are up to ~2 GHz and ~5.2 GHz, respectively.

4. Summary

In summary, to the best of our knowledge, we experimentally demonstrate the first NOM-p based FTN signaling over OWC. In order to apply the advanced FSD to a large-size multi-carrier FTN system, we have further proposed MB-NOM-p technology and have also verified its improved BER performance when ICI is severe. All the results have indicated the superior performance of the proposed scheme, including PAPR reduction, simple channel estimation and equalization, the additional coding gain and the improved tolerance to narrow-bandwidth filtering.

5. References

[1] Y. Wang et al., *Photonics. J.*, vol. 7, pp. 1-7, 2015.
[2] I. Darwazeh et al., *PTL*, vol. 26, pp. 352–355, 2014.
[3] Z. Hu et al., *JLT*, 2019 (Early Access).
[4] W. Ozan et al., *CSNDSP,* pp. 1-6, 2018.
[5] M McGuire et al., *GC Wkshps*, 2016.
[6] J. Huang et al., *Photonics. J.*, vol. 8, pp. 1–9, 2016.
[7] F. Li et al., *Opt. Exp.*, vol. 22, pp. 8742–8748, 2014.
[8] T. Xu et al., *Commun. Lett.*, vol. 17, pp. 1964–1967, 2013.
[9] Y. Hong et al., *OFC*, M3A.6, 2016.
[10] Z. Feng et al., *PTL*, vol. 27, pp. 1507–1510, 2015.